Supplementary Information

Electrodeposited SiO_2 film: a promising interlayer of highly active Ti electrode for oxygen evolution reaction

Lian-Kui Wu,[a,b] Xin-Yu Liu,[a] Ji-Ming Hu,[a,*]

[a] Department of Chemistry, Zhejiang University, Hangzhou 310027, China

[b] College of Materials Science and Engineering, Zhejiang University of Technology, Hangzhou 310014, China

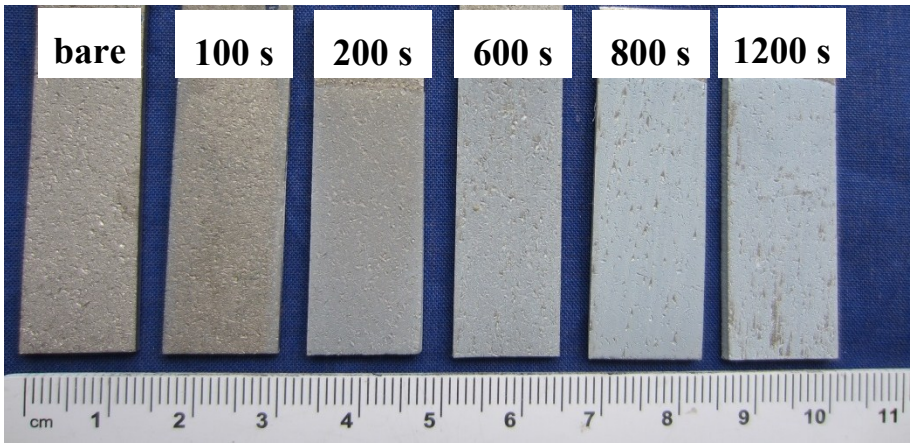

Figure S1 Optical images of e-SiO_2 films deposited on Ti substrates for different deposition time at -1.6 V vs. Ag/AgCl.

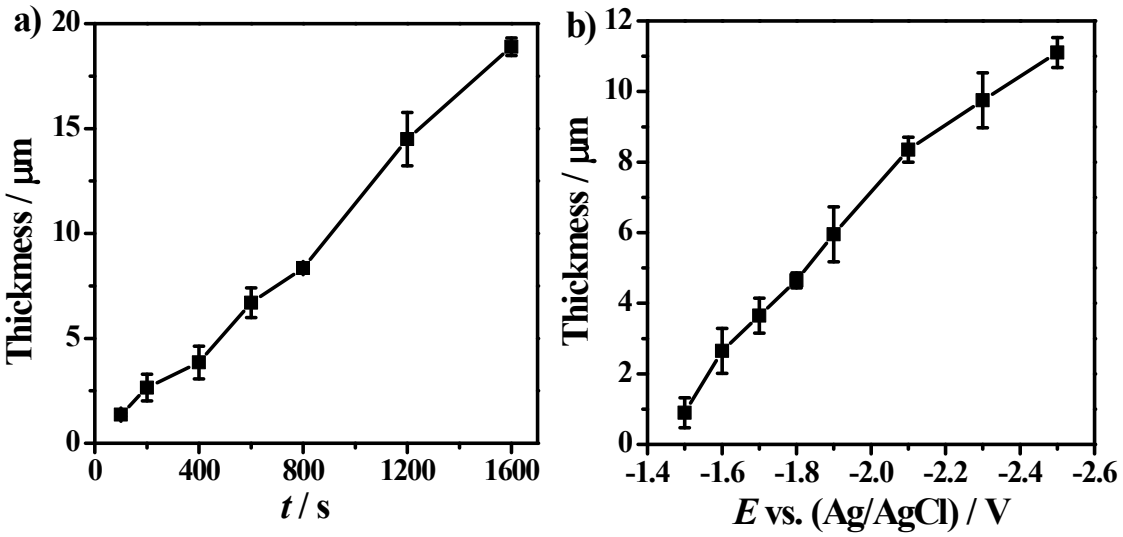

Figure S2 (a) Electrodeposition time dependence of thickness of the e-SiO_2 films fabricated on polished Ti substrate at -1.6 V vs. Ag/AgCl; (b) Electrodeposition potential dependence of thickness of the e-SiO_2 films prepared on polished Ti substrate for 200 s. The error bars are derived from one sample by three independent measurements.

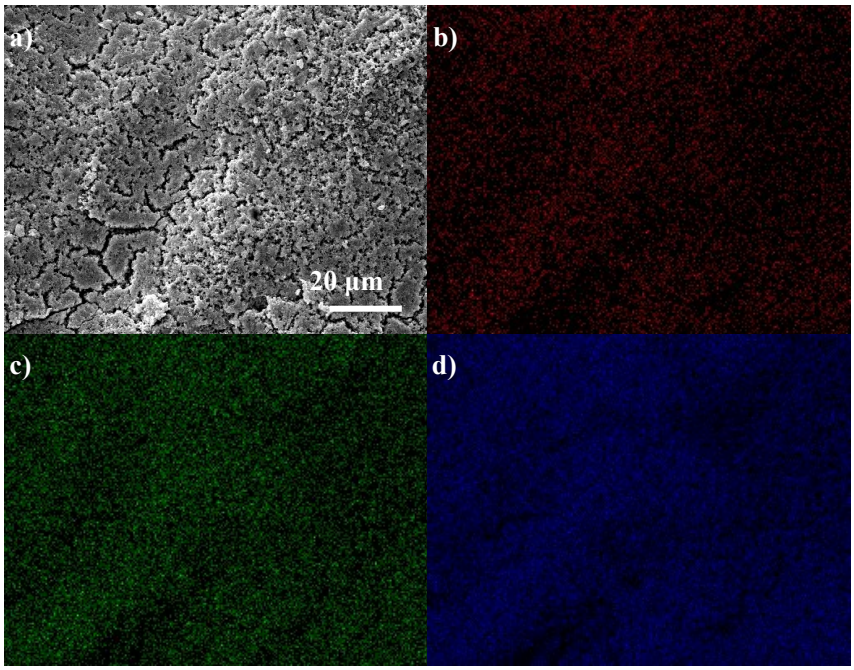

Figure S3 A SEM image of Ti/e-SiO_2/IrO_2 electrode with e-SiO_2 interlayer prepared at -1.6 V for 200 s (a) and the corresponding energy dispersive X-ray maps of the same sample showing the dispersion O (b), Si (c), Ir(d).

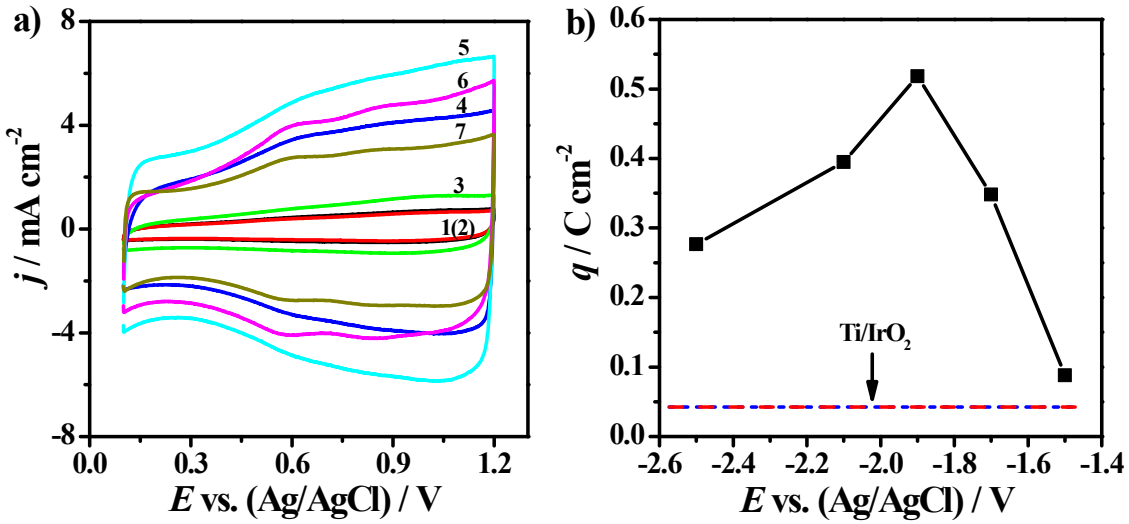

Figure S4 Cyclic voltammograms (a) and integrated voltammetric charges (b) of IrO_2 electrodes prepared at Ti substrates before (1) and after dip-coating with silica film (2) and Ti/e-SiO_2/IrO_2 electrodes with e-SiO_2 interlayer prepared at different potentials for 200 s: -1.5 V (3), -1.7 V (4), -1.9 V (5), -2.1 V (6) and -2.5 V (7). The measurements were carried out in 0.5 mol L^{-1} H_2SO_4 solution at a scan rate of 20 mV s^{-1}.

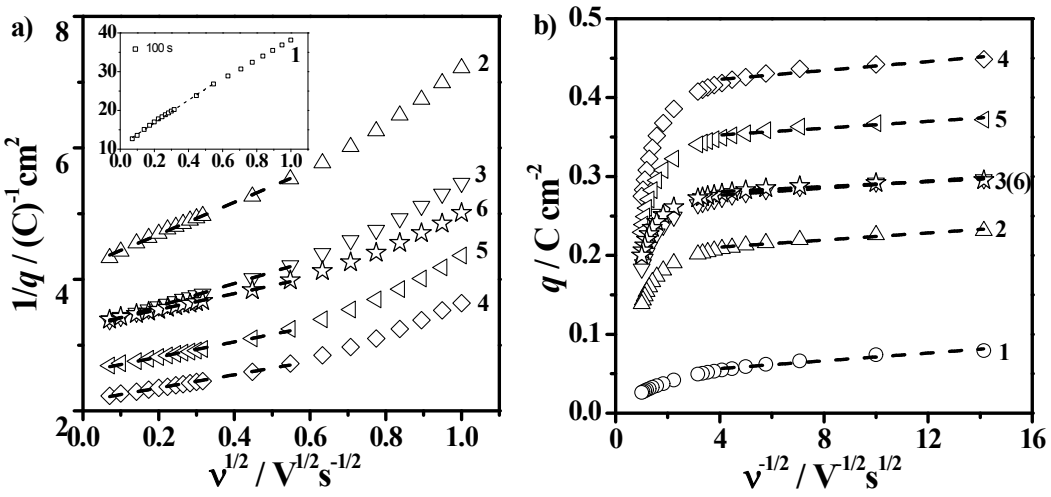

Figure S5 Extrapolation of integrated voltammetric charge, q^*, to $v \rightarrow 0$ (a) and $v \rightarrow \infty$ (b). Data are measured at Ti/E-SiO_2/IrO_2 electrodes with E-SiO_2 interlayer prepared at -1.6 V for different electrolysis time: 100 s (1), 200 s (2), 400 s (3), 800 s (4), 120 s (5) and 1600 s (6). Dash line: linear region.

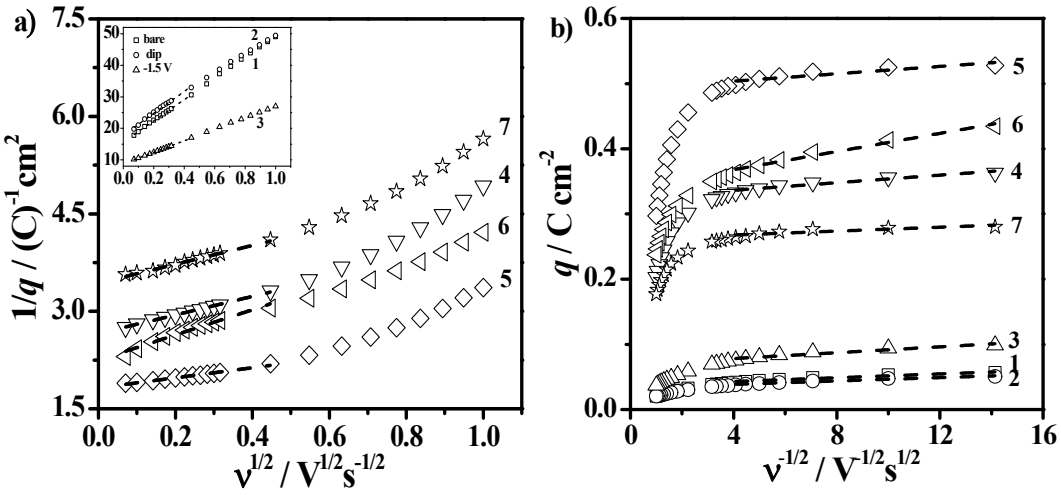

Figure S6 Extrapolation of integrated voltammetric charge, q^*, to $v \rightarrow 0$ (a) and $v \rightarrow \infty$ (b). Data were measured at Ti/E-SiO_2/IrO_2 electrodes with SiO_2 interlayer prepared at various deposition potential for 200 s: bare (1), dip coating (2), -1.5 V (3), -1.7 V (4), -1.9 V (5), -2.1 V (6) and -2.5 V (7). Dash line: linear region.

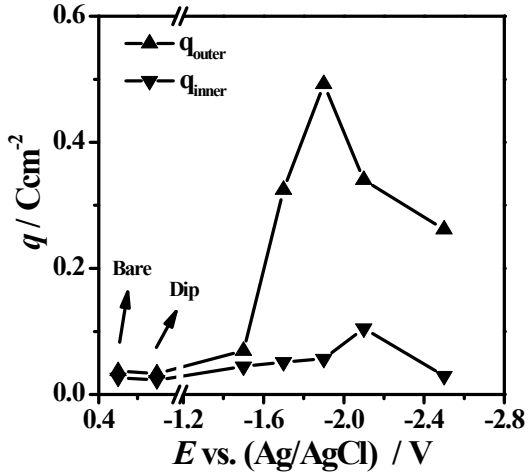

Figure S7 The change of q_{inner} (down-triangle) and q_{outer} (up-triangle) for Ti/e-SiO_2/IrO_2 electrodes with e-SiO_2 interlayer prepared at different potentials for 200 s.

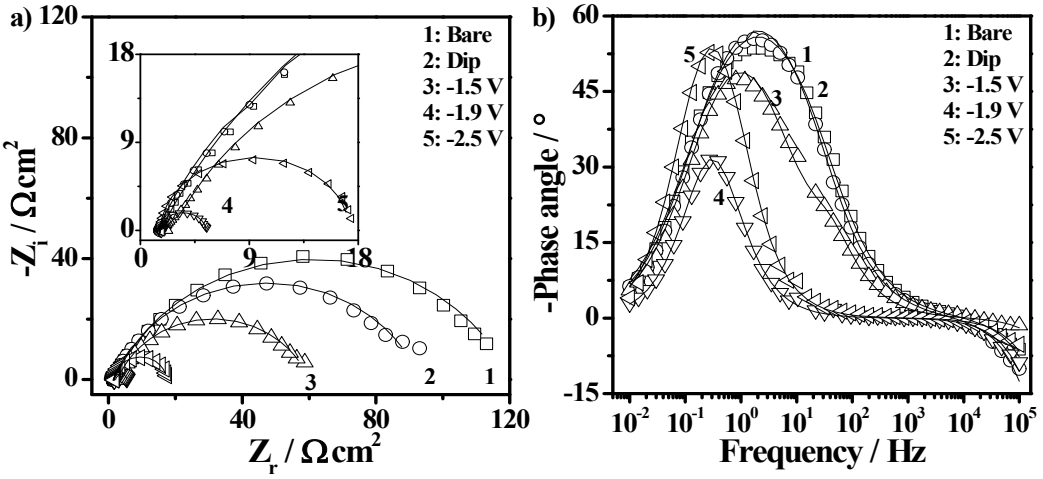

Figure S8 Nyquist diagrams (a) and Bode plots (b) of Ti/E-SiO_2/IrO_2 electrodes with the SiO_2 interlayer prepared at various potentials for 200 s: bare (1), dip coating (2), -1.5 V (3), -1.9 V (4) and -2.5 V (5). The measurements were conducted in 0.5 mol L^{-1} H_2SO_4 solution at 1.30 V. Dash line: Fitting results.

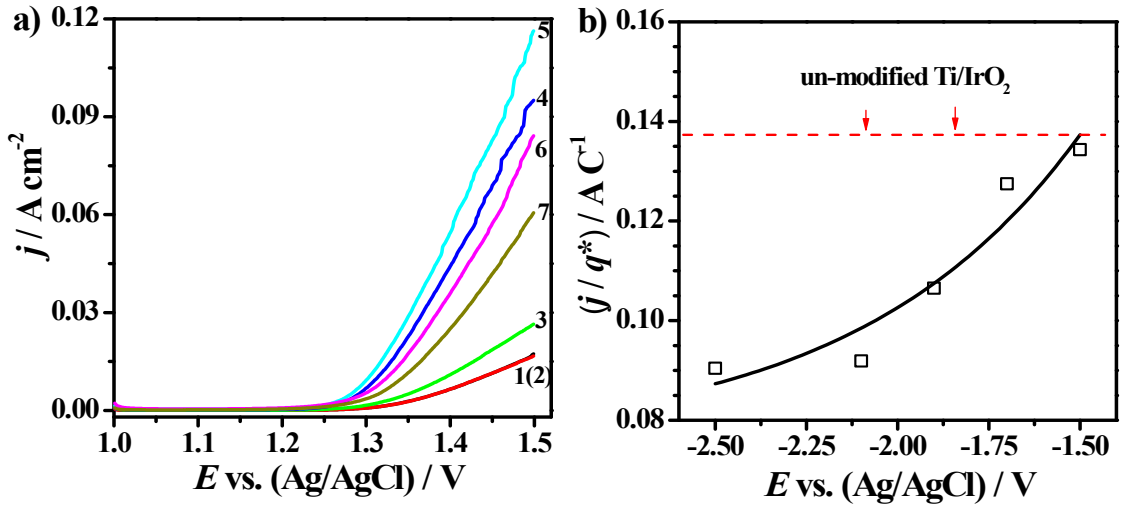

Figure S9 Steady-state polarization curves (a) and derived j/q^* curves (b) of the Ti/IrO_2 electrode (1), Ti/dip-coated SiO_2/IrO_2 electrode (2), and $Ti/e\text{-}SiO_2/IrO_2$ electrodes with e-SiO_2 interlayer prepared at different potentials for 200 s: -1.5 V (3), -1.7 V (4), -1.9 V (5), -2.1 V (6) and -2.5 V (7). The data were collected in 0.5 mol L^{-1} H_2SO_4 solution at scan rate of 1.0 mV s^{-1}.

Table S1 Values of the equivalent circuit parameters for Ti/E-SiO_2/IrO_2 electrodes in 0.5 mol L^{-1} H_2SO_4 at 1.30 V

Electrode	R_s / Ωcm²	$L \times 10^6$ / Hcm⁻²	$Q_{dl,I}$ / Ω⁻¹cm⁻²Sⁿ	$n1$	$R_{ct,I}$ / Ωcm²	$Q_{dl,O}$ / Ω⁻¹cm⁻²Sⁿ	$n2$	$R_{ct,O}$ / Ωcm²	$C_{dl,O}$ / Fcm⁻²	$C_{dl,I}$ / Fcm⁻²	$C_{dl,Total}$ / Fcm⁻²
Bare	1.44	3.53E-7	0.0212	0.774	5.62	0.0118	0.828	107.8	0.00503	0.00716	0.0122
Dip	1.42	4.96E-7	0.0254	0.782	1.42	0.0135	0.804	89.11	0.0051	0.00827	0.0134
-1.5V	1.51	2.17E-7	0.0161	0.888	1.06	0.0198	0.793	56.26	0.00785	0.00902	0.0169
-1.7V	1.53	4.55E-7	0.103	0.895	0.0933	0.175	0.939	5.243	0.158	0.0595	0.217
-1.9V	1.57	4.83E-7	0.182	0.908	0.0505	0.257	0.961	3.81	0.244	0.112	0.356
-2.1V	1.78	2.93E-7	0.163	0.830	0.0922	0.165	0.959	11.01	0.156	0.0681	0.224
-2.5V	1.62	2.95E-7	0.108	0.809	0.526	0.153	0.968	15.7	0.145	0.0515	0.197
100s	1.94	3.81E-7	0.0417	0.705	1.43	0.0172	0.837	69.52	0.00881	0.0102	0.0190
200s	1.43	3.63E-7	0.0950	0.747	0.157	0.0820	0.918	19.9	0.0674	0.0220	0.0894
400s	1.58	3.00E-7	0.0984	0.793	0.110	0.133	0.928	12.61	0.117	0.0296	0.146
800s	1.48	3.56E-7	0.178	0.875	0.0991	0.208	0.934	5.385	0.189	0.0987	0.287
1200s	1.58	2.96E-7	0.158	0.828	0.0468	0.170	0.958	7.959	0.159	0.0569	0.216
1600s	1.45	3.71E-7	0.138	0.709	0.0964	0.136	0.954	9.699	0.125	0.0228	0.148